International Journal of Nanomedicine

Dovepress
open access to scientific and medical research

Open Access Full Text Article

ORIGINAL RESEARCH

Ginsenoside Rh2-Based Multifunctional Liposomes for Advanced Breast Cancer Therapy

Chao Hong[1,2,*], Anni Wang[1,*], Jiaxuan Xia[1], Jianming Liang[1,3], Ying Zhu[1], Dan Wang[1,4], Huaxing Zhan[4], Chunbo Feng[5], Xinnan Jiang[5], Junjie Pan[6], Jianxin Wang[1,7]

[1]Department of Pharmaceutics, School of Pharmacy, Fudan University & Key Laboratory of Smart Drug Delivery, Ministry of Education, Shanghai, 201203, People's Republic of China; [2]School of Pharmacy, Shanghai University of Traditional Chinese Medicine, Shanghai, 201203, People's Republic of China; [3]Institute of Tropical Medicine, Guangzhou University of Chinese Medicine, Guangzhou, 510006, People's Republic of China; [4]Xiamen Ginposome Pharmaceutical Co., Ltd, Xiamen, 361026, People's Republic of China; [5]R&D Center, Shanghai Jahwa United Co., Ltd, Shanghai, 200082, People's Republic of China; [6]Department of Cardiology, Huashan Hospital, Fudan University, Shanghai, 200040, People's Republic of China; [7]Institute of Integrated Chinese and Western Medicine, Fudan University, Shanghai, 200040, People's Republic of China

*These authors contributed equally to this work

Correspondence: Junjie Pan; Jianxin Wang, Email junjie112@163.com; jxwang@shmu.edu.cn

Background: Most solid tumors are not diagnosed and treated until the advanced stage, in which tumors have shaped mature self-protective power, leading to off-target drugs and nanomedicines. In the present studies, we established a more realistic large tumor model to test the antitumor activity of a multifunctional ginsenoside Rh2-based liposome system (Rh2-lipo) on advanced breast cancer.

Methods: Both cholesterol and PEG were substituted by Rh2 to prepare the Rh2-lipo using ethanol-water system and characterized. The effects of Rh2-lipo on cell uptake, penetration of the tumor spheroid, cytotoxicity assay was investigated with 4T1 breast cancer cells and L929 fibroblast cells. The 4T1 orthotopic-bearing large tumor model was established to study the targeting effect of Rh2-lipo and inhibitory effect of paclitaxel loaded Rh2-lipo (PTX-Rh2-lipo) on advanced breast tumors.

Results: Rh2-lipo exhibit many advantages that address the limitations of current liposome formulations against large tumors, such as enhanced uptake in TAFs and tumor cells, high targeting and penetration capacity, cytotoxicity against TAFs, normalization of the vessel network, and depletion of stromal collagen. In in vivo study, PTX-Rh2-lipo effectively inhibiting the growth of advanced breast tumors and outperformed most reported PTX formulations, including Lipusu® and Abraxane®.

Conclusion: Rh2-lipo have improved drug delivery efficiency and antitumor efficacy in advanced breast cancer, which offers a novel promising platform for advanced tumor therapy.

Keywords: nanomedicine, tumor microenvironment, chemotherapy, tumor-associated fibroblast

Introduction

Cancer remains a highly fatal disease in the world. The past three decades have witnessed a great expansion of research in the field of cancer nanomedicine. Various nanoparticles that include lipid-based nanoparticles, polymeric nanoparticles, and inorganic nanoparticles have been developed for targeted delivery of therapeutic nucleic acids,[1] chemotherapeutic agents,[2] or immunotherapeutic agents to tumors.[3] The advantage of using nanomedicines to treat cancer is that they can effectively target and deliver drugs to the tumor site,[4] reducing side effects and improving treatment efficiency. In addition, nanomedicines have a controlled release function, allowing drugs to be slowly released at the tumor site, reducing the frequency of dosing, and improving patient compliance.[5] However, there is a large body of literature describing different nanoparticles as potential cancer therapies, yet only a handful has been US Food and Drug Administration (FDA) approved.[6]

The tumor microenvironment (TME) is well known for its important role in cancer development and metastasis[7–9] Various cells in the TME, especially stromal cells, including tumor-associated fibroblasts (TAFs), collagen, and endothelial cells, form a physical barrier within tumors to inhibit penetration of therapeutic nanoparticles and secrete

Received: 13 December 2023
Accepted: 7 March 2024
Published: 20 March 2024

Graphical Abstract

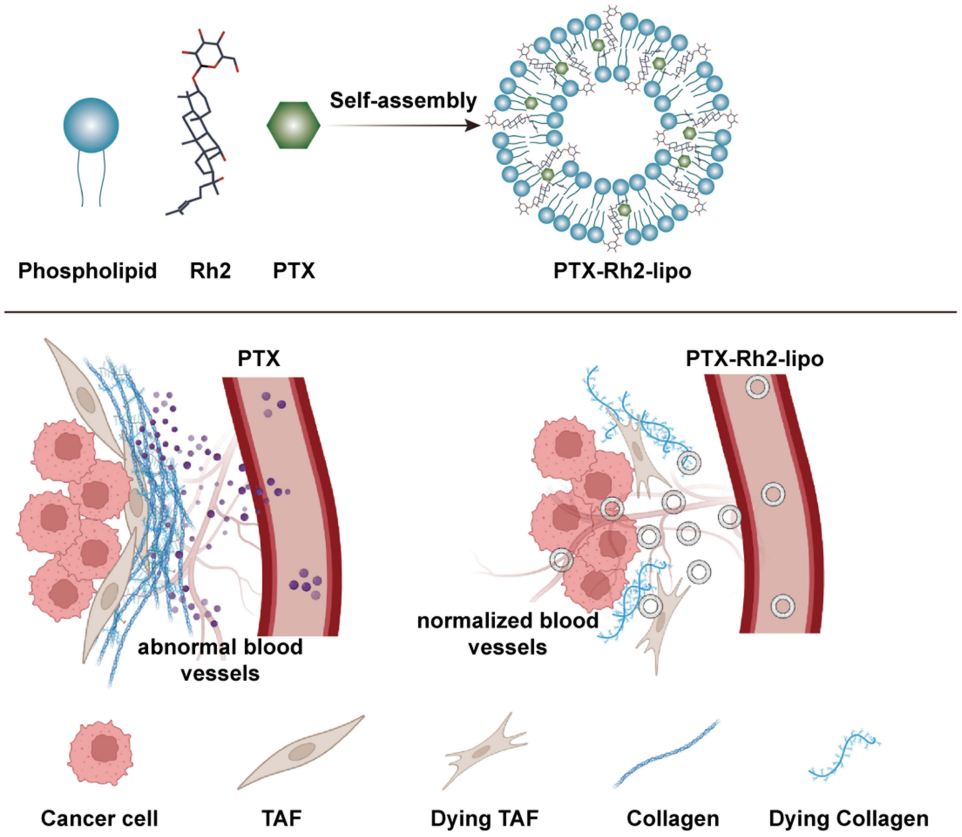

growth-inducing cytokines and growth factors to facilitate the survival of tumor cells, which finally results in the resistance of nanochemotherapy[7,9] Evidence has shown that in the early stages of tumor growth, the composite of the TME is much simpler and far from shaping self-protective mechanisms.[10] When tumor growth bursts into the advanced stage, the tumor-vessel TME transforms into the stroma-vessel type in which the stroma executes the function of tumor cell protection,[10,11] including enhancing tumor cell proliferation and invasion,[8,9] and contributes to immune suppression.[8,12,13] Studies have shown that TAFs are a major component of the TME and can represent up to approximately 80% of stromal cells in TME,[14] and causes drug delivery deficiencies and off-target effects.[15] However, mostly reported tumor targeting strategies were aimed at early-stage tumors by taking small tumors (50–150 mm^3) as animal models to evaluate their treatment efficacy, which were not similar to the real situation in clinics.[16] Compared to the commonly used small tumor model, the large tumor model (400–600 mm^3)[10] was much more realistic to reflect the clinical status. Therefore, as mentioned above, a large tumor model faces challenges that are difficult to treat and raise a higher demand for drug delivery, which should possess high infiltration capacity and efficiency to remodel the TME, particularly overcoming the crosstalk between the stroma and tumor cells.[17]

Liposome, a specific type of nanocarrier, has passed into clinical use with different formulations. Compared to other nano-delivery systems, liposomes offer advantages such as biocompatibility, versatility in drug loading, targeted delivery, and prolonged circulation,[18] making them a highly promising nano delivery system in various biomedical applications. Our previous studies have shown that ginsenoside Rh2-based liposomes coloaded with paclitaxel (PTX-Rh2-lipo) have outstanding antitumor ability in small tumor models.[19–23] In Rh2-lipo, both cholesterol and PEG were substituted by Rh2, which works as membrane stabilizer, long-circulating stealther, active targeting ligand, and chemotherapy adjuvant at the same time. Firstly, Rh2 could keep the stability of liposomes and avoid the shortcomings caused by cholesterol.[19,20]

Secondly, Rh2-lipo showed a specifically prolonged circulation behavior in the blood.[20,23] Thirdly, the accumulation of the liposomes in the tumor was significantly enhanced by the interaction of glucose transporter of tumor cells with Rh2.[20,23] Fourth, Rh2-lipo could remodel the tumor structure, including the expression and distribution of vessels, TAFs and collagens.[19,20] When tested in an 4T1 breast orthotopic small cancer model, paclitaxel loaded Rh2-lipo (Rh2-PTX-lipo) were quite efficient in tumor suppression but caused few systematic toxicities.[20] Overall, in contrast to conventional wooden liposomes, PTX-Rh2-lipo is a potential nanomedicine with multiple functions, which has great potential to overcome the dilemma in advanced tumor therapy. Therefore, in this study, we established a large breast tumor model to evaluate the effect of Rh2-lipo and PTX-Rh2-lipo in treating advanced cancer.

Materials and Methods

Materials

Ginsenoside Rh2, PTX, Lipusu® (paclitaxel liposome for injection), and Abraxane® (paclitaxel protein-bound particles for injectable suspension) were provided by Xiamen Ginposome Pharmatech Co., Ltd. (Xiamen, China). Egg yolk lecithin (EYL) and cholesterol were purchased from AVT Pharmaceutical Co., Ltd. (Shanghai, China). Coumarin 6 (C6), Hoechst 33,342, and near-infrared dye 4-chlorobenzenesulfonate salt (DiD) were received from Fanbo Biochemicals (Beijing, China). 5-(dimethyl-thiazol-2-yl)-2,5-diphenyl-tetrazolium bromide (MTT) was purchased from Sigma (St. Louis, MO, USA).

Cell Culture

Cells were obtained from the Cell Bank of the Chinese Academy of Sciences (Shanghai, China). 4T1 cells were cultured in RPMI-1640 (Gibco) supplemented with 10% fetal bovine serum (FBS) at 37°C in a humidified 5% CO_2 atmosphere. L929 cells were cultured in DMEM (Gibco) supplemented with 10% FBS at 37°C in a humidified 5% CO_2 atmosphere.

Preparation and Characterization of Liposomes

Liposomes were prepared by a thin-film hydration method as previously reported.[19] Briefly, ginsenoside Rh2 liposomes (Rh2-lipo) were made of EYL and Rh2 (10:3, mass ratio), while conventional liposomes (C-lipo) were prepared with the same lipid composition (EYL: cholesterol =10:3, mass ratio). First, all lipid materials were dissolved in chloroform and ethanol (1:1, volume ratio), followed by rotary evaporation to form a lipid film using a ZX-98 rotary evaporator (LOOYE, China) at 50°C. After the thin film was hydrated with water at 50°C for 30 min, the liposomal suspension was then subjected to a probing sonication process in an ice bath for 10 min at 300 W with a sequence of 5 s of sonication and 5 s of rest using a sonicator (Sonics & Materials, Inc., 20 kHz). PTX-, C6-, and DiD-loaded liposomes were prepared by the same method described above with EYL: PTX, EYL: C6, EYL: DiD ratios of 10:1, 1000:1, and 1000:1, respectively.

The particle size and ζ-potential of liposomes were measured by a dynamic light scattering detector (Zetasizer, Nano ZS, Malvern, UK). The morphology of PTX-loaded liposomes was detected by transmission electron microscopy (TEM, Tecnai G2 F20 S-Twin, FEI, USA). The encapsulation efficiency (EE) and the loading efficiency (LE) of PTX were measured using a previously reported method.[19]

Cellular Uptake

Liposomal cellular uptake was evaluated in 4T1 cells and L929 cells. 4T1 cells were seeded in 12-well plates at a density of 1×10^5 cells per well. After 12 h, C6-labeled C-lipo and Rh2-lipo were added to 4T1 cells at a final C6 concentration of 500 ng/mL. After 2 h incubation at 37°C, cells were stained with Hoechst 33,342 and then washed three times with PBS. Finally, the samples were visualized by fluorescence microscopy (Leica, DMI4000D, Germany). The study of liposomal cellular uptake in L929 cells was the same as above.

Penetration of the Tumor Spheroid

Tumor spheroids were prepared to investigate the penetration capability of Rh2-lipo in tumors. First, 1% (w/v) low melting point agarose was added to a 96-well plate. Then, a mixture of L929 cells and 4T1 cells was seeded on agarose-coated plates at a density of 4×10^3 per well (4T1: L929=1:3) and incubated until spheroids formed. The tumor spheroids were incubated with C6-labeled C-lipo or Rh2-lipo for 4 h (n=3). The spheroids were then rinsed with PBS and subjected to confocal microscopy (ZEISS, 710, LSM, Germany).

Animals and Ethics Approval

Female BALB/c mice aged 4–6 weeks were purchased from Sino-British SIPPR/BK Lab Animal and housed under pathogen-free conditions in the Assessment and Accreditation of Laboratory Animal Care (AAALAC)-accredited animal facilities at School of Pharmacy, Fudan University.

All animal work was done according to the approvals from the Institutional Animal Care and Use Committees (IACUC) of School of Pharmacy, Fudan University and complied with the ethical regulations and humane endpoint criteria of the National Institutes of Health's Guidelines for the Care and Use of Laboratory Animals (approval number: 2019–03-YJ-WJX-01).

In vivo Animal Imaging

The 4T1 orthotopic-bearing large tumor mouse model was established to study the targeting effect of Rh2-lipo. When the volume of tumors reached approximately 450 mm^3, 4T1 orthotopic-bearing tumor mice were intravenously injected via the tail with DiD-loaded C-lipo or Rh2-lipo. 24 h later, the mice were sacrificed after heart perfusion with saline. Tumors were harvested and fixed in 4% formaldehyde overnight and dehydrated in 15% and 30% sucrose solutions until subsidence. Then, tumors were frozen and cut into 15 μm slices. DAPI was used for nuclear staining. The distribution of fluorescence was visualized using confocal scanning laser microscopy.

In vivo Antitumor Efficacy

The antitumor efficacy of PTX-Rh2-lipo was evaluated by monitoring tumor growth in a 4T1 orthotopic-bearing large tumor model (female, approximately 18 g body weight). When the volume of tumors reached approximately 450 mm^3, the mice were randomly assigned to each group, which were administered Lipusu®, Abraxane®, and PTX-Rh2-lipo with PTX content at 10 mg/kg body weight, and Rh2 and Rh2-lipo with Rh2 content at 30 mg/kg body weight. All the formulations were intravenously injected via tail veins every other day for 21 days. The tumor sizes and body weights were measured every three days and calculated as $A \times B^2/2$, where A was the largest diameter and B was the smallest. Finally, the mice were sacrificed by cervical dislocation under anesthesia. Tumors were excised and the organs were collected.

To further evaluate the antitumor effect of PTX-Rh2-lipo on the animals, the tumors were fixed with 4% (v/v) paraformaldehyde in PBS (pH 7.4) and sectioned into 5 μm slices. Apoptotic and nonapoptotic cells in tumor tissues were histologically evaluated with the terminal deoxynucleotidyl transferase-mediated nick end labeling (TUNEL) assay using a commercial apoptosis detection kit (Promega, Madison, WI). Vessels and TAFs were characterized by rabbit anti-mouse CD31 and rabbit anti-mouse α-SMA and then treated with Alexa Fluor 647-conjugated goat anti-rabbit antibody. Nuclei were counterstained with DAPI (Vector Laboratories, Inc., Burlingame, CA). All commercial binding reagents were diluted according to the manufacturer's recommendation. Images were taken using fluorescence microscopy (Nikon, Tokyo, Japan). Three randomly selected microscopic fields were quantitatively analyzed using ImageJ software.

Collagen in tumor tissues was detected by Masson's trichrome assay. The tumor slides were stained using a Masson Trichrome Kit (Saint Louis, MO, USA) according to the manufacturer's instructions. Images were taken using light microscopy. Three randomly selected microscopic fields were quantitatively analyzed using ImageJ software.

Table 1 Characterization of Different PTX Liposomes (n = 3; Mean ± SD)

Liposome	PTX-C-Lipo	PTX-Rh2-Lipo
Size (nm)	130.01±2.46	99.03±3.22
PDI	0.26±0.011	0.27±0.014
ZP (mV)	−21.86±0.82	−39.21±1.03
EE (%)	90.1±1.6	91.3±2.1
LE (%)	6.4±0.2	5.6±0.3

Abbreviations: PDI, polydispersity index; ZP, zeta potential; EE, encapsulation efficiency; LE, loading efficiency.

Statistical Analysis

Values were presented as the mean ± SD as indicated and were analyzed using GraphPad Prism 6.0 (GraphPad Software, CA, USA). Differences were assessed using one-way analysis of variance followed by the Newman-Keuls post hoc test for multiple groups and Student's *t* test between two groups.

Results and Discussion

Characterization of Liposomes

The mean particle sizes, Polydispersity index (PDI), and ζ-potentials of two liposomal formulations are listed in Table 1. Notably, liposomes modified with Rh2 exhibited a significantly smaller particle size and higher zeta potential compared to conventional cholesterol liposomes. Other crucial factors associated with the encapsulation and stabilization abilities of both types of liposomes, such as PDI, EE, and LE, were found to be quite similar. Moreover, as shown in Figure 1, the TEM observation revealed that PTX-Rh2-lipo exhibited a homogeneous spheroidal morphology with moderate dispersion.

Cellular Uptake of Rh2-Lipo in TAFs and Tumor Cells

The growth and development of tumor cells often create a high interstitial fluid pressure in the advanced stage, leading to poor drug intratumoral infiltration. To demonstrate the transfer of Rh2-lipo in TAFs and tumor cells, we selected L929 fibroblasts and 4T1 breast cancer cells and conducted an uptake assay. As shown in Figure 2A and B, confocal

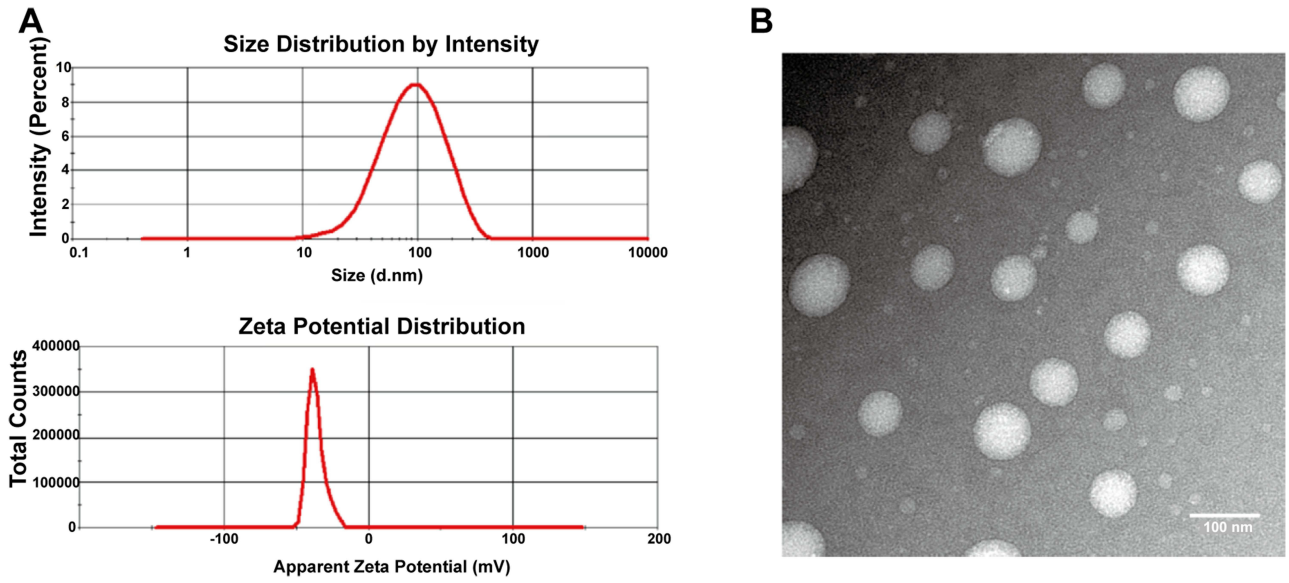

Figure 1 Characterization of the liposomes. (**A**) Size and zeta potential of PTX-Rh2-lipo. (**B**) TEM image of PTX-Rh2-lipo. Scale bar = 100 nm.

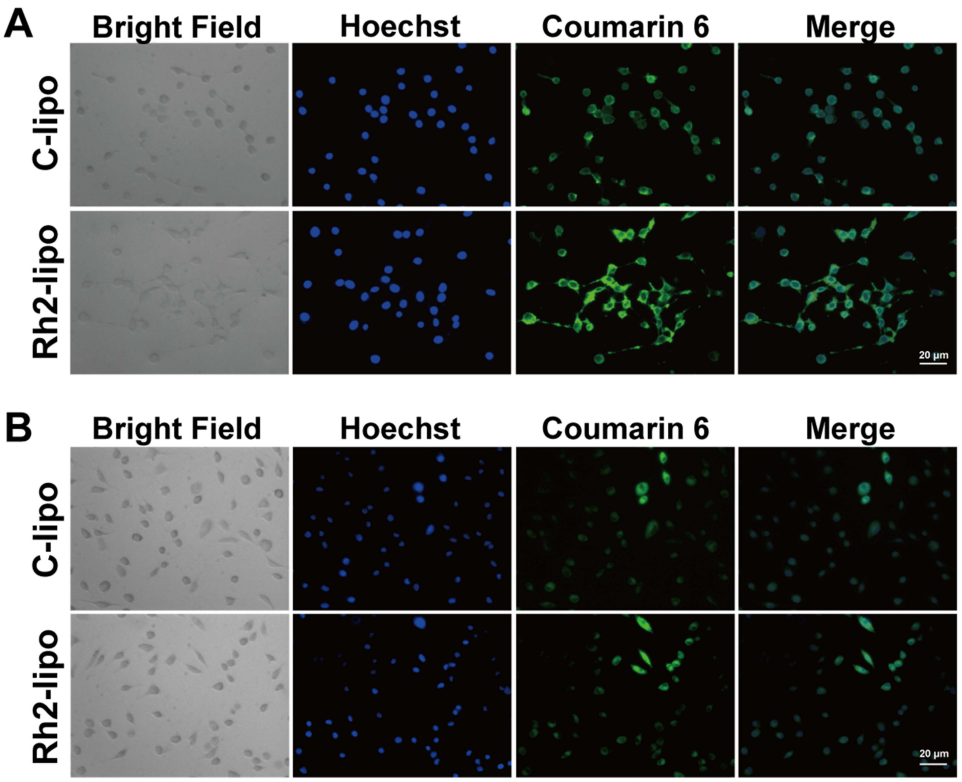

Figure 2 The confocal fluorescence images of cellular uptake on L929 cells (**A**) and 4T1 cells (**B**). Scale bar = 20 μm.

fluorescence images clearly indicate that the fluorescence intensity of C6-labeled Rh2-lipo on 4T1 cells and L929 cells is significantly stronger than that of labeled C-lipo, suggesting an enhanced cellular uptake of Rh2-lipo. The improved cellular uptake of Rh2-lipo in L929 cells may result from the specific interaction between Rh2-lipo and glucose receptors on the surface of cells, which has been observed and proven in tumor cells in previous studies.[20]

However, the enhanced uptake of liposome in L929 cells could potentially hinder the uptake of tumor cells within the TME, due to the presence of TAFs, which serve as barriers shielding tumor cells from liposome uptake. In order to accurately assess the transfer and penetration efficacy of Rh2-lipo in tumors, it is essential to construct a multicellular model that better mimics the complexity of the TME.

Penetration of Rh2-Lipo in vitro/In vivo

To evaluate the penetrating ability of Rh2-lipo in vitro, a tumor spheroid model mixed with 4T1 and L929 cells was established to imitate the native tumor environments.[24]

As shown in Figure 3A, in the cultured tumor spheroids with diameters of 300–400 μm, the penetration distance of Rh2-lipo (53.87 μm) was much deeper than that of C-lipo (27.04 μm), indicating that Rh2-lipo have a higher efficiency of penetration. We hypothesized that the recruitment and transfer of Rh2-lipo to tumor spheroids occurred through the utilization of glucose receptors present on the surface of various cells. Once the outer layer cells of the spheroids became saturated with Rh2-lipo, the internal receptors continued to attract liposomes, facilitating further infiltration.

To further validate the penetration capability of Rh2-lipo in advanced cancer, we established a large tumor model in mice. The results showed in Figure 3B and C demonstrate that after 8 hours of circulation within the body, Rh2-lipo exhibited a higher fluorescence intensity in the tumor tissue compared to C-lipo. This observation indicates a significantly enhanced accumulation of liposomes and a stronger ability to penetrate the large tumor.

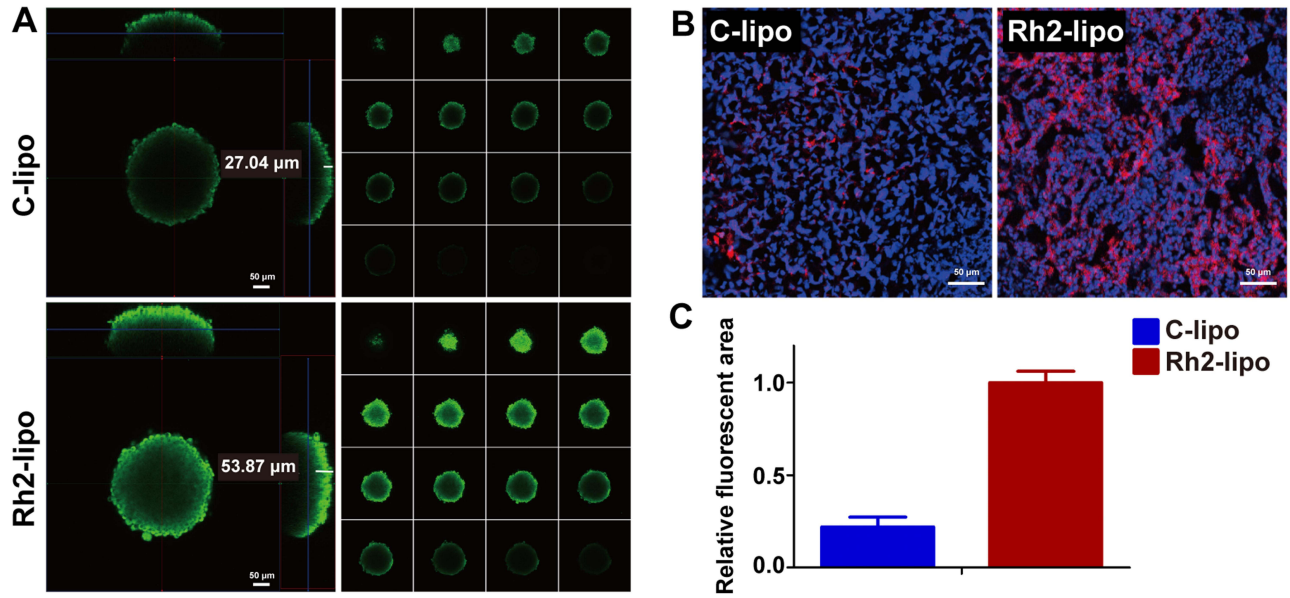

Figure 3 Assessment of intratumoral penetration ability using tumor spheroids treated with C-lipo and Rh2-lipo. (**A**) Representative images of C-lipo and Rh2-lipo in vitro. Scale bar = 50 μm. (**B**) Representative images of C-lipo and Rh2-lipo in vivo. Scale bar = 50 μm. (**C**) Quantitative analysis of the penetration depth in the advanced tumor.

In vivo Antitumor Efficacy

To investigate the effectiveness of liposomes in combating advanced tumors in vivo, we conducted experiments on 4T1-orthotopic tumor-bearing mice. Once the tumor volume reached 450 mm3, indicating the advanced stage,[10] the mice were treated with different formulations containing a PTX dosage of 10 mg/kg. To compare the efficiency of PTX-loaded Rh2 liposomes against advanced breast cancer, we selected two commercially available PTX nano-formulations, Lipusu® and Abraxane®. Abraxane®, which is an albumin-based formulation of PTX, is widely recognized as the most effective PTX formulation worldwide. Lipusu®, also known as paclitaxel liposome for injection, is composed of PTX solubilized in liposomes formed from lecithin and cholesterol. It has been approved in China for clinical chemotherapy treatment for the past 20 years.

As shown in Figure 4, Abraxane® showed a moderate inhibitory effect on tumor growth. However, PTX-Rh2-lipo exhibited the highest antitumor efficacy against advanced tumors. Other groups, including Lipusu®, did not show any significant inhibition of large tumor growth. Interestingly, although Rh2-lipo has stronger penetration ability in the tumors, it cannot kill 4T1 tumor cells alone. The best antitumor effect only exerted by the combination of Rh2-lipo with PTX, which was consistent with our previous study,[20] indicating that Rh2-lipo primarily serves as a delivery vehicle for PTX to enhance its antitumor properties here.

There is no significant difference in the blood indicators of mice among the different treatment groups (Table S1). However, the weights of PTX-Rh2-lipo and Abraxane® obviously decreased (Figure 4B), while the other groups showed no loss of weight. Abraxane® is known for its toxicity by good absorption in tumors and other healthy tissues, and we proposed that the toxicity of PTX-Rh2-lipo was aggravated due to its increased cellular uptake in the whole body by glucose receptors. Further studies specifically targeting drug metabolism and potential long-term toxicity effects were on the way.

To observe the therapeutic effects of liposomes in vivo more intuitively, a TUNEL staining experiment was performed. As shown in Figure 4C and D, PTX-Rh2-lipo exhibited the highest fluorescence intensity compared with Abraxane® and Lipusu®, indicating that Rh2-lipo increased the apoptosis inducing efficacy of PTX on tumor cells in vivo.

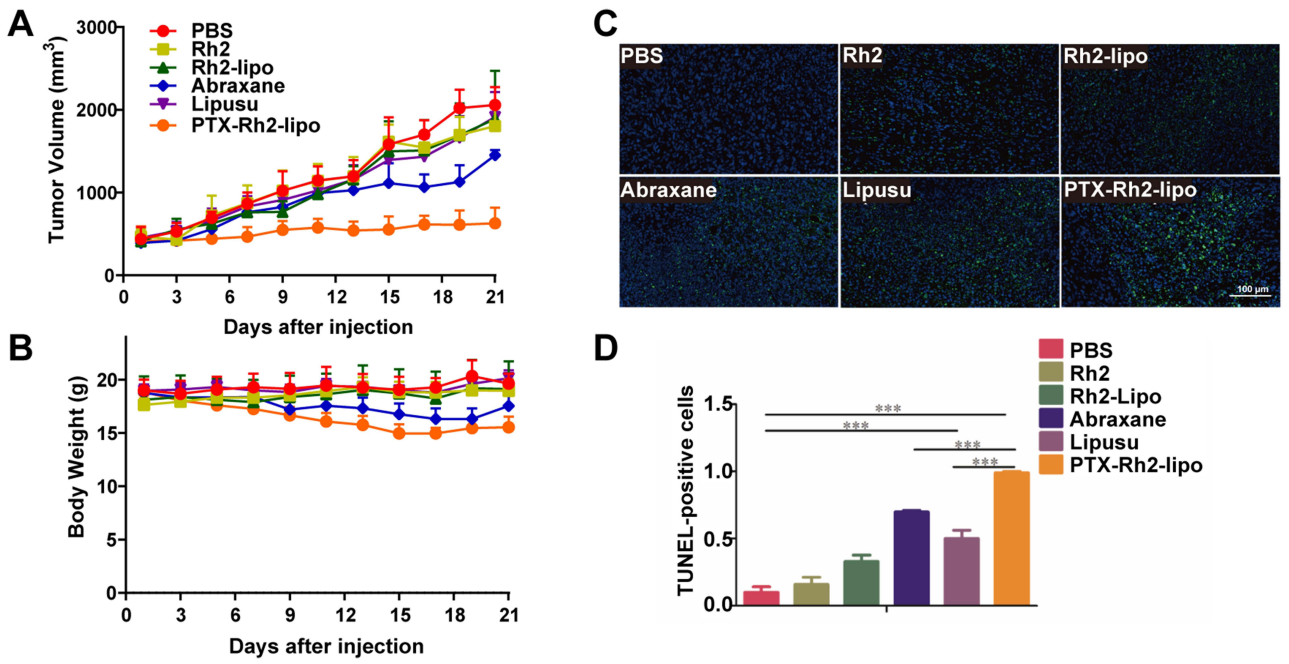

Figure 4 4T1-orthotopic tumor growth curve in the different groups. (**A**) Tumor growth curve during of 4T1 tumor-bearing mice after i.v. injection of different preparations at a dose of 10 mg/kg (n=6, mean ± SD). (**B**) Body weight variations over the course of the drug treatment regimen (n=6, mean ± SD). (**C**) TUNEL analysis of advanced tumors. Blue: cell nuclei, DAPI. Green: apoptotic cells. Scale bar = 100 μm. (**D**) TUNEL-positive cells intensity in advanced tumors (n=3, mean ±SD, ***p < 0.001).

The Modulation of TME

Evidence has demonstrated that the stromal vessel-type TME, particularly TAFs, serves as barriers to impede the penetration of antitumor therapeutics into the central region of tumors.[9] Accordingly, we conducted investigations to examine how Rh2-lipo influences the remodeling of the TME, focusing on the distribution of vessels and the expression of TAFs and collagen.

The vessels, stained with green fluorescence, were distributed randomly in the tumor with a thin and elongated morphology that can greatly impede the penetration of drugs from vessels. As shown in Figure 5A, the Rh2, Rh2-lipo, and PTX-Rh2-lipo groups exhibited a decrease in vessel density, indicating a stronger inhibitory effect on angiogenesis compared to Lipusu®. The fluorescence intensity of PTX-Rh2-lipo resembled that of Abraxane®, suggesting that this formulation induced the most effective normalization of the tumor blood vessel network.

TAFs, visualized by α-SMA staining in Figure 5B, exhibited a similar trend as the vessels. PTX-Rh2-lipo demonstrated the most pronounced anti-TAF effect, implying that this formulation not only exhibited higher uptake in TAFs but also exerted cytotoxicity towards them, ultimately eliminating their protective role in advanced tumors.

It was reported that TAFs could stimulate the TME to release and express more collagen (Masson's trichrome staining)[25] to provide highways for invading tumor cells.[26] In Figure 5C, obviously, compared to overspread and thick fibrous structures in other groups, PTX-Rh2-lipo showed the best antitumor effect by inhibiting collagen production.

In brief, the above results demonstrated that TME in an advanced tumor model was completely remodeled and reversed by PTX-Rh2-lipo treatment, indicating that Rh2-lipo was not only effective against cancers in an earlier period but also had potential in treating advanced cancers.

To determine the safety and immunological regulatory effects of the formulations, tumor-bearing mice were sacrificed, and their organs were harvested. Sections of organs were made to verify discernible tissue damage. As shown in Figure 5D and E, varying levels of tissue necrosis were observed in the major organs, attributed to the invasion of inflammatory cells. Notably, immune-induced inflammatory damage was observed in the organs of all groups, except for the PTX-Rh2-lipo treated group. The Rh2-lipo and free Rh2 groups also exhibited reduced inflammatory damage, suggesting a potential role for ginsenoside Rh2 in modulating the systemic immune response.[20]

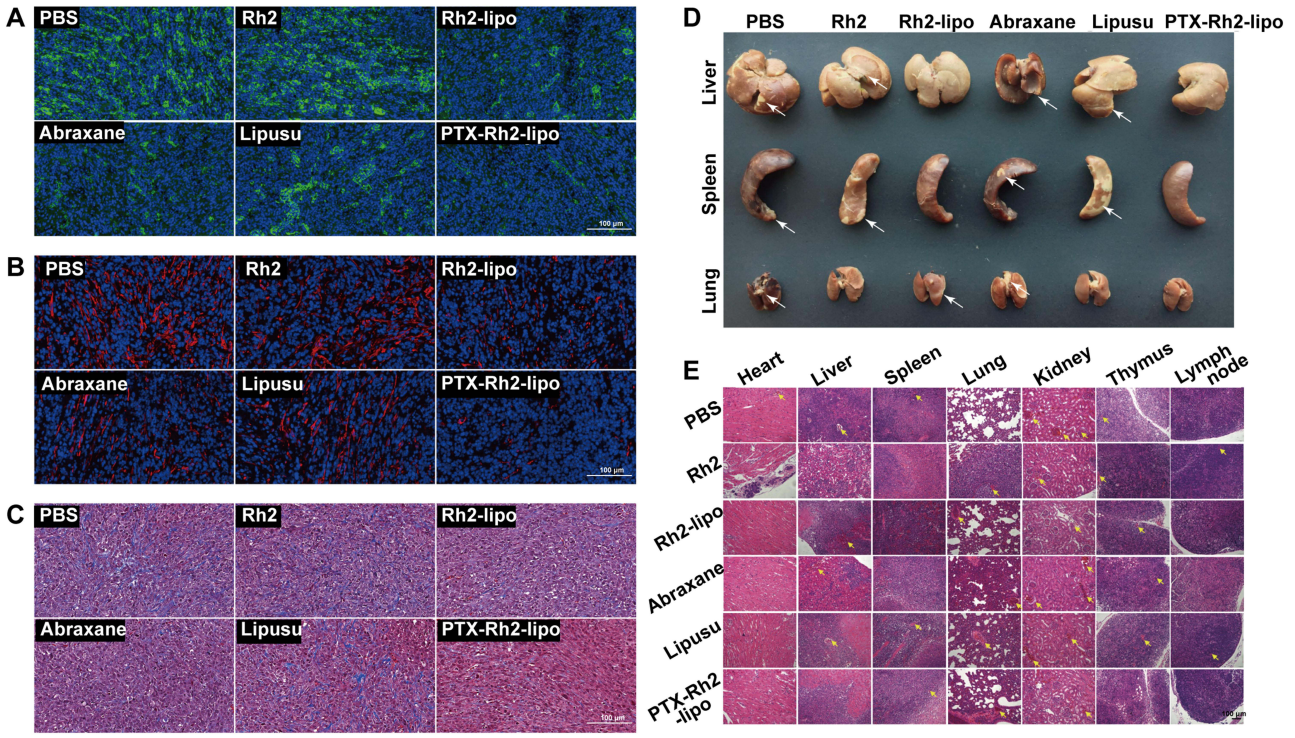

Figure 5 (**A**) Vessels in 4T1 tumors were stained with CD31 antibody (green) and normalized in structure and reduced in expression after treatment. Scale bar = 100 μm. (**B**) TAFs in tumors were stained with α-SMA antibody (red) and significantly decreased after treatment. Scale bar = 100 μm. (**C**) Collagen fibers were stained with Masson's Trichrome and significantly decreased after treatment. Scale bar = 100 μm. (**D**) and (**E**) Rh2-lipo decreased the inflammatory storm in organs (immune-induced inflammatory damage were highlighted by white arrows) and sections (tissue necrosis were highlighted by yellow arrows). Scale bar = 100 μm.

Conclusion

In this study, a more realistic tumor model in the advanced stage was established, in which the tumor-vessel TME had already transformed into a stroma-vessel type TME. The complex TME network executes the function of tumor cell protection, leading to nanochemotherapy resistance. Here, a novel and unique Rh2 liposomal system was established, overcoming the dilemma in advanced tumor therapy. Rh2-lipo exhibit many advantages that address the limitations of current liposomes, such as enhanced uptake in TAFs and tumor cells, high targeting and penetration capacity, cytotoxicity against TAFs, normalization of the vessel network, and depletion of stromal collagen. Rh2 serves as an active ingredient to synergically enhance the efficacy of chemo drugs by remodeling the tumor-associated microenvironment and finally effectively inhibits the growth of advanced tumors. Although only 4T1 breast tumors were tested as the model cancer in this study, the Rh2-lipo could be extended to other advanced cancer models.

Funding

This work was supported by the National Natural Science Foundation of China (No. 82074277), and the Development Project of Shanghai Peak Disciplines-Integrated Medicine (No. 20180101).

Disclosure

Co-authors Dan Wang and Huaxing Zhan are employed by Xiamen Ginposome Pharmaceutical Co., Ltd. Co-author Xinnan Jiang is employed by Shanghai Jahwa United Co., Ltd. The other authors have no conflicts of interest in this work.

References

1. Deng T, Hasan I, Roy S., et al. Advances in mRNA nanomedicines for malignant brain tumor therapy. *Smart Mater Med*. 2023;4:257–265. doi:10.1016/j.smaim.2022.11.001

2. Wu W, Pu Y, Shi J. Nanomedicine-enabled chemotherapy-based synergetic cancer treatments. *J Nanobiotechnol*. 2022;20(1):4. doi:10.1186/s12951-021-01181-z
3. Yi Y, Yu M, Li W, et al. Vaccine-like nanomedicine for cancer immunotherapy. *J Control Release*. 2023;355:760–778. doi:10.1016/j.jconrel.2023.02.015
4. Zhang Y, Zhang H, Zhao F, et al. Mitochondrial-targeted and ROS-responsive nanocarrier via nose-to-brain pathway for ischemic stroke treatment. *Acta Pharm Sin B*. 2023;2:1.
5. Sun L, Liu H, Ye Y, et al. Smart nanoparticles for cancer therapy. *Signal Transduct Target Ther*. 2023;8(1):418. doi:10.1038/s41392-023-01642-x
6. Liu P, Chen G, Zhang J. A review of liposomes as a drug delivery system: current status of approved products, regulatory environments, and future perspectives. *Molecules*. 2022;27(4):1372. doi:10.3390/molecules27041372
7. Binnewies M, Roberts EW, Kersten K, et al. Understanding the tumor immune microenvironment (TIME) for effective therapy. *Nat Med*. 2018;24(5):541–550. doi:10.1038/s41591-018-0014-x
8. Chhabra Y, Weeraratna AT. Fibroblasts in cancer: unity in heterogeneity. *Cell*. 2023;186(8):1580–1609. doi:10.1016/j.cell.2023.03.016
9. Wang M, Zhao J, Zhang L, et al. Role of tumor microenvironment in tumorigenesis. *J Cancer*. 2017;8(5):761–773. doi:10.7150/jca.17648
10. Miao L, Newby JM, Lin CM, et al. The binding site barrier elicited by tumor-associated fibroblasts interferes disposition of nanoparticles in stroma-vessel type tumors. *ACS nano*. 2016;10(10):9243–9258. doi:10.1021/acsnano.6b02776
11. Winkler J, Abisoye-Ogunniyan A, Metcalf KJ, et al. Concepts of extracellular matrix remodelling in tumour progression and metastasis. *Nat Commun*. 2020;11(1):5120. doi:10.1038/s41467-020-18794-x
12. Zhang H, Yue X, Chen Z, et al. Define cancer-associated fibroblasts (CAFs) in the tumor microenvironment: new opportunities in cancer immunotherapy and advances in clinical trials. *Mol Cancer*. 2023;22(1):159. doi:10.1186/s12943-023-01860-5
13. Sahai E, Astsaturov I, Cukierman E, et al. A framework for advancing our understanding of cancer-associated fibroblasts. *Nat Rev Cancer*. 2020;20(3):174–186. doi:10.1038/s41568-019-0238-1
14. Fernández-Nogueira P, Fuster G, Gutierrez-Uzquiza Á, et al. Cancer-associated fibroblasts in breast cancer treatment response and metastasis. *Cancers*. 2021;13(13):3146. doi:10.3390/cancers13133146
15. Khawar IA, Kim JH, Kuh HJ. Improving drug delivery to solid tumors: priming the tumor microenvironment. *J Control Release*. 2015;201:78–89. doi:10.1016/j.jconrel.2014.12.018
16. Schachtschneider KM, Schwind RM, Newson J, et al. The oncopig cancer model: an innovative large animal translational oncology platform. *Front Oncol*. 2017;7:190. doi:10.3389/fonc.2017.00190
17. Xu M, Zhang T, Xia R, et al. Targeting the tumor stroma for cancer therapy. *Mol Cancer*. 2022;21(1):208. doi:10.1186/s12943-022-01670-1
18. Nsairat H, Khater D, Sayed U, et al. Liposomes: structure, composition, types, and clinical applications. *Heliyon*. 2022;8(5):e09394. doi:10.1016/j.heliyon.2022.e09394
19. Hong C, Wang D, Liang J, et al. Novel ginsenoside-based multifunctional liposomal delivery system for combination therapy of gastric cancer. *Theranostics*. 2019;9(15):4437. doi:10.7150/thno.34953
20. Hong C, Liang J, Xia J, et al. One stone four birds: a novel liposomal delivery system multi-functionalized with ginsenoside Rh2 for tumor targeting therapy. *Nanomicro Lett*. 2020;12:1–18.
21. Xia J, Zhang S, Zhang R, et al. Targeting therapy and tumor microenvironment remodeling of triple-negative breast cancer by ginsenoside Rg3 based liposomes. *J Nanobiotechnol*. 2022;20(1):414. doi:10.1186/s12951-022-01623-2
22. Zhu Y, Liang J, Gao C, et al. Multifunctional ginsenoside Rg3-based liposomes for glioma targeting therapy. *J Control Release*. 2021;330:641–657. doi:10.1016/j.jconrel.2020.12.036
23. Chen C, Xia J, Ren H, et al. Effect of the structure of ginsenosides on the *in vivo* fate of their liposomes. *Asian J Pharm Sci*. 2022;17(2):219–229. doi:10.1016/j.ajps.2021.12.002
24. Lu H, Stenzel MH. Multicellular Tumor Spheroids (MCTS) as a 3D *In Vitro* Evaluation Tool of Nanoparticles. *Small*. 2018;14(13):e1702858. doi:10.1002/smll.201702858
25. McCarthy JB, El-Ashry D, Turley EA. Hyaluronan, cancer-associated fibroblasts and the tumor microenvironment in malignant progression. *Front Cell Dev Biol*. 2018;6:48. doi:10.3389/fcell.2018.00048
26. Nissen NI, Karsdal M, Willumsen N. Collagens and Cancer associated fibroblasts in the reactive stroma and its relation to Cancer biology. *J Exp Clin Cancer Res*. 2019;38(1):1–12. doi:10.1186/s13046-019-1110-6